

SUMMARY OF THE INVESTIGATION OF LOW TEMPERATURE, LOW DOSE RADIATION EFFECTS ON THE V-4Cr-4Ti ALLOY — L. L. Snead, S. J. Zinkle, D. J. Alexander, A. F. Rowcliffe, J. P. Robertson, and W. S. Eatherly (Oak Ridge National Laboratory)

OBJECTIVE

This paper presents a summary of the results obtained from the HFBR-V1 through -V4 capsules which investigated the effects of low-dose, low-temperature neutron irradiation on the mechanical behavior of V-4Cr-4Ti alloys.

SUMMARY

Experimental details, raw data, method of analysis and results are presented for the low-temperature, low-dose HFBR-V1 through V4 irradiation experiments conducted at ORNL on V-4Cr-4Ti specimens (U.S. Fusion Program Heat #832665). Four separate capsules were irradiated in the V-15 and V16 In-Core Thimbles of the High Flux Beam Reactor at the Brookhaven National Laboratory to doses of 0.1 or 0.5 dpa at temperatures between 100 and 505°C. Testing included microhardness, electrical resistivity, tensile properties, and Charpy impact properties.

PROGRESS AND STATUS

Experimental Details

The V-4Cr-4Ti alloy used in this study was procured from Teledyne Wah Chang Albany (TWCA) and designated the U.S. Fusion Program Heat #832665. The interstitial impurity concentrations in this alloy were approximately 300 wppm O, 85 wppm N, and 80 wppm C [1,2]. All materials were annealed by TWCA at 1050°C for 1 or 2 hours with some receiving 50% cold work [2]. All materials used in the four irradiation capsules were nominally the same chemistry, although the specimens were machined from different plate stock provided by Argonne National Laboratory to ORNL (cf. Table 1). Specimens were electro-discharge machined (EDM) by the same machine shop into miniature Charpy vee-notch (CVN) impact specimens, type SS-3 miniature sheet tensile specimens, and transmission electron microscopy (TEM) disks. Following machining, all samples were ultrasonically cleaned in acetone and isopropyl alcohol and given a final heat treatment in vacuum (pressure $<10^{-7}$ Torr) at the conditions listed in Table 1. The CVN specimen dimensions were $3.3 \times 3.3 \times 25.4$ mm with a 30° notch, 0.67 mm deep with a 0.08 mm root radius. The notch was oriented for crack growth perpendicular to the rolling direction (L-T orientation). Following the final heat treatment, some Charpy specimens were fatigue pre-cracked (PCVN's) by cyclic loading in 3-point bending in stroke control, so the load would shed automatically as the crack extended. The final load was approximately 130 N, and the final crack length to specimen width ratio (a/W) was nominally 0.5. The SS-3 miniature sheet tensile specimens ($0.76 \times 1.52 \times 7.6$ mm gage section) were oriented in the longitudinal orientation (parallel to the rolling direction). The final grain size in both the CVN and SS-3 specimens was approximately 16 μ m. TEM disks (3 mm diameter by 0.25 mm thick) were included in the HFBR-V3 and V4 capsules only. TEM disks for samples irradiated in the V1 and V2 capsules were obtained by cutting slices from irradiated CVN specimens following impact testing. Details regarding the specimen series number, initial and final thermomechanical treatment of the alloy and other information on the materials used in this study are given in Table 1. Note that the majority of materials irradiated, and all those for which postirradiation mechanical property results are presented in this summary, are for the 2 h, 1000°C heat treatment.

Table 1. Identification of materials and annealing condition.

Capsule	SS-3 Tensile Series ID & Specimen HT	1/3 PCVN Series ID & Specimen HT	1/3 MCVN Series ID & Specimen HT	TEM Disks Series ID & Specimen HT
V 1	WH (2h @ 1000°C)	WB (2h @ 1000°C)	WB (2h @ 1000°C)	
V 2	WH (2h @ 1000°C)	WB (2h @ 1000°C)	WB (2h @ 1000°C)	
V 3	WH (2h @ 1000°C) ST (2h @ 1000°C) ST (2h @ 900°C)	QC (2h @ 1000°C) QC (2h @ 900°C)	QC (2h @ 1000°C)	ND (1h @ 900°C) ND (1h @ 1000°C)
V 4	ST (2h @ 1000°C) ST (2h @ 900°C)	QC (2h @ 1000°C)		ND (1h @ 900°C) ND (1h @ 1000°C)

Specimen Series ID	ORNL ID Plate/Sheet	ANL ID Plate/Sheet	Prior Conditioning	Plate Thickness
WH	N40	Plate D	1050°C (1 h) + 50% CR (TWCA)	0.040"
ST	S40	2/96	1050°C (1 h) + 50% CR (TWCA)	0.040"
WB	M150	Plate A	1050°C (2 h) (TWCA)	0.150"
QC	Q250	Plate A (annealed)	1050°C (2 h) (TWCA)	0.250"
ND	N40-10		1000°C(1 h) + 40% CR (ORNL)	0.010"

The irradiation capsules were designed for insertion into the core thimble position in the High Flux Beam Reactor at the Brookhaven National Laboratory. Each capsule consisted of several gas-gapped subcapsules containing the samples. Variations in the sample temperature in the different subcapsules was achieved by varying the gas gap between the subcapsules and the inside of the external capsule, which was in contact with the core coolant water. A cross sectional schematic of a subcapsule is shown in Fig. 1. The subcapsule bodies were electro-discharge machined from either Type 6061-T6 aluminum or remelted V-4Cr-4Ti. Each subcapsule typically contained 8 machined or pre-cracked CVN and 4 SS-3 tensile specimens. After the samples were loaded, a Type 304 stainless steel roll pin (a spring) was lightly hammered into place to ensure that the CVN specimens were in good thermal contact with the subcapsule wall. Each subcapsule used one type-K thermocouple embedded into a Charpy specimen which monitored temperature throughout the irradiation. This thermocouple was located in Charpy #1 (see Fig. 1). In subcapsule 2 of the HFBR-V1 capsule, a second thermocouple was inserted into Charpy #3 to detect any asymmetry in heat flow distribution. As described later, the temperatures for the two thermocouples agreed within 8°C. For the case of subcapsule 1 of HFBR-V3, 21 tensile specimens filled the subcapsule and the thermocouple was placed into the body of the aluminum holder. Due to the numerous heat flow interfaces, it is likely that the differences between the thermocouple reading and the actual sample temperatures were greater in this case than for the subcapsules containing the Charpy specimens. It could also be argued that there would be a larger sample-to-sample difference for the tensile specimens in subcapsule 1, although the measured hardness values were nearly identical for the SS-3's indicating that temperature differences were not significant.

All samples and capsule components were ultrasonically cleaned in isopropyl alcohol and acetone prior to capsule assembly. After the capsule was assembled and the ~33 meter umbilical Type 8000 aluminum tubing was welded in place, the capsule was helium leak checked using a helium

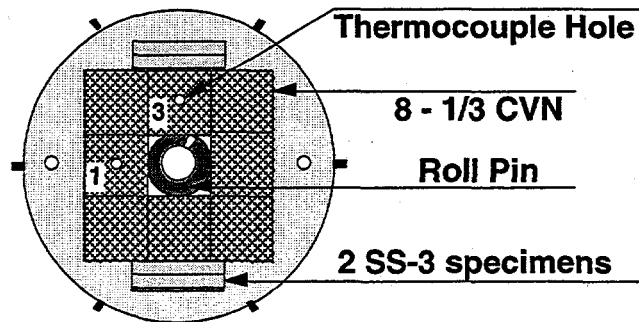


Fig. 1. Cross section of subcapsule for HFBR-V1 through V4 experiments. The numbers 1 and 3 refer to Charpy specimen positions which contained thermocouples.

mass spectrometer. The capsule was then evacuated using an oil-free turbomolecular pump and back-filled with ultra high purity helium to 15 psig. This procedure was repeated three times. Between the first and second evacuation cycles the capsule was baked out to 400°C under vacuum. After the final backfill to 15 psig the pressure was monitored continuously from time of assembly until the end of the irradiation. At no time did the capsule pressure reach atmospheric pressure during the irradiation. However, for the V1 and V2 capsules a small helium leak caused the capsule pressure to decrease during irradiation. This was corrected during irradiation by valving off the irradiation capsules, and then evacuating and back-filling with helium the gas handling manifolds (which were not removed after capsule construction.) Once the manifold was purged and backfilled with UHP helium, the capsule was repressurized with helium to 15 psig.

The four separate irradiation capsules of this study, HFBR-V1 through V4, were irradiated in the High Flux Beam Reactor between May 1995 and October 1996. Experiments HFBR-V1 and V2 were irradiated in the in-core thimble V15 while HFBR-V3 and V4 were irradiated in the symmetric V16 thimble. The HFBR-V1 and V2 capsules were first inserted near the bottom of the core (prior to startup) and began irradiation in this position. These two capsules were approximately 18 cm in length and held 4 and 5 subcapsules, respectively (cf. Table 2). HFBR-V1 was raised to the center of the core after 76 h of the 544 h irradiation. HFBR-V2 was raised to the center of the core after 94 h of the 507 h irradiation. HFBR-V3 received 510 h irradiation in the center of the V-16 thimble, and HFBR-V4 was irradiated for 100 h in the center of the V-16 thimble. The HFBR-V3 and V4 capsules were approximately 23 cm in length, and were held in the center of the core during their entire irradiation period. Each of the V3 and V4 capsules contained 6 subcapsules operating at different temperatures.

At the time of these irradiations the HFBR was operating at 30 MW_{th} power. In our earlier reports on the HFBR V1 and V2 capsules [3,4], the results from a 1976 dosimetry campaign were used to obtain estimates of the fast and thermal neutron fluences, and the nominal damage level for the V1-V2 capsules was reported to be 0.4 dpa. Greenwood and Ratner have recently compiled flux values from three separate dosimetry experiments of the HFBR V-15 In Core thimble that were conducted between 1976 and 1996 using bare and cadmium-covered flux monitors [5]. From the data analysis (scaled to a reactor power of 30 MW_{th}), it was concluded that the most reliable value for the thermal flux ($E < 0.5$ eV) was $1.23 \pm 0.10 \times 10^{18}$ n/m²-s and the fast flux ($E > 0.11$ MeV) was $2.64 \pm 0.26 \times 10^{18}$ n/m²-s. It is noted that no dosimetry has been conducted on the V-16 thimble in which the HFBR V3-V4 capsules were irradiated. It is assumed that the fast flux is essentially the same as V-15 due to its symmetric position. Also, based on Monte Carlo calculations it is assumed that the center 40 cm of 55 cm core is flux-invariant. Each of the capsules V1-V3 were irradiated to estimated fast ($E > 0.1$ MeV) and thermal fluences of $\sim 5.0 \pm 0.2 \times 10^{24}$ n/m² and 2.3×10^{24} n/m²,

Table 2. Variation in subcapsule temperatures during irradiation.

Capsule ID (Subcapsule)	Temperature Range, °C (average)	Comment
HFBR V1 (1)	107-108 (108)	+
HFBR V1 (2)	195-201 (198) 203-209 (206)	Position #1 CVN(fig 1)* Position #3 CVN(fig 1)*
HFBR V1 (3)	272-278 (275)	*,+
HFBR V1 (4)	204-210 (207)	*,+
HFBR V2 (1)	227-236 (232)	+
HFBR V2 (2)	232-242 (237)	+
HFBR V2 (3)	194-206 (200)	+
HFBR V2 (4)	197-208 (203)	+
HFBR V2 (5)	107-115 (111)	+
HFBR V3 (1)	159-161 (160)	+
HFBR V3 (2)	267-268 (268)	+
HFBR V3 (3)	259-262 (260)	+
HFBR V3 (4)	322-325 (324)	+
HFBR V3 (5)	305-309 (307)	+
HFBR V3 (6)	410-417 (414)	+
HFBR V4 (1)	105	+
HFBR V4 (2)	160	+
HFBR V4 (3)	256	+
HFBR V4 (4)	294	+
HFBR V4 (5)	391	+
HFBR V4 (6)	504	+

*Temperature increased monotonically throughout irradiation

+Thermocouple in CVN Position 1 (see Fig. 1)

respectively, which produced a calculated [5] damage level in vanadium of 0.5 dpa. Because of the movement of the V1 and V2 capsules from a point near the bottom of the core to the core centerline it can be assumed that these capsules received somewhat (<10%) lower fluence than did the V3 subcapsule which was irradiated at the core centerline throughout the irradiation. The thermal neutron fluence in the V1-V3 capsules would have produced a calculated chromium concentration of 0.1% Cr. The V4 experiment was irradiated for 100 h at the center of the core for an estimated fast and thermal fluence of $0.95 \pm 0.1 \times 10^{24}$ and $0.44 \pm 0.04 \times 10^{24}$ n/m², respectively, corresponding to a dose of about 0.1 dpa.

During irradiation, the temperatures of the samples were recorded continuously. Table 2 gives the range in temperature recorded by the thermocouples for each experiment. The temperature variations for the V1-V3 subcapsules were always less than 12°C, most of which is accounted for by movement of the V1 and V2 capsules to the center of the core during the irradiation. The V4 capsule had essentially no temperature variation (due to the shorter period of irradiation). The temperature for the V1 capsule slowly increased throughout the irradiation. The reason for this increase is unknown. Because a monotonic temperature increase did not occur in the subsequent capsules (V2-V4), thermocouple decalibration due to transmutation appears unlikely. Also of note in Table 2 is the slight difference in measured temperature between the CVN position 1 and 3 thermocouples in the second subcapsule of V1. Both thermocouples were embedded in Charpy samples to essentially the same depth and yielded about an 8°C difference in measured temperature which tracked each other during the irradiation. From inspection of

Fig.1, this may be explained by the added thermal interfaces sample #3 has between the sample and the subcapsule housing tube. The heat generated in sample #3 would have flowed through the adjacent Charpy samples or through two stacked SS-3's prior to reaching the subcapsule housing.

Results and Discussion

Hardness

Microhardness was measured using a Buehler microhardness tester with a Vickers pyramidal indenter. Data were taken at 500 g, 1 kg and 2 kg loads. Similar hardness values were obtained at all three loads. The data presented here are from the 500 g loads and represent mean values of between 8 and 20 indents each. Samples were prepared by dry sanding the surface of the vanadium specimen. To insure hydrogen pick-up did not affect the hardness results, a full series of hardness tests at 0.5 to 2 kg loads were performed on both sanded and non-sanded, unirradiated vanadium. No difference in hardness was observed. The indents were placed either in the end tab region of the SS-3 sheet tensile specimen or on the side of Charpy specimen. The hardness measurements on the Charpy specimens were taken following impact testing. Sample edges were avoided in all cases.

Figure 2 gives the results of all hardness data taken on the irradiated vanadium specimens at a load of 500 g. The unirradiated hardness values are also listed in Fig. 2. It was observed that the subtle differences in the materials processing used in this study (Table 1) had a measurable effect on the unirradiated hardness. For example, the ST and WH series tensile specimens had unirradiated hardness values of 144.8 ± 0.9 and 134.2 ± 0.9 VHN while the WB and QC series Charpy samples had 150.9 ± 2.1 and 139.9 ± 0.4 VHN, respectively. The hardness errors quoted here and plotted in Fig. 2 refer to one standard error. The temperature error given in Fig. 2 is a combination of the temperature variation during the irradiation and an assumed discrepancy between the sample temperature and the recorded thermocouple temperature of 5°C .

From Fig. 2 it is seen that hardening occurs as the irradiation temperature is increased from $\sim 100^\circ\text{C}$ to $200\text{-}300^\circ\text{C}$, particularly for the 0.5 dpa irradiation. While there is significant scatter for the compiled V1-V3 data, the point at which the room temperature hardness is maximized appears to occur at a higher irradiation temperature for the 0.5 dpa irradiation ($\sim 300^\circ\text{C}$) compared to the 0.1 dpa irradiation ($\sim 150^\circ\text{C}$).

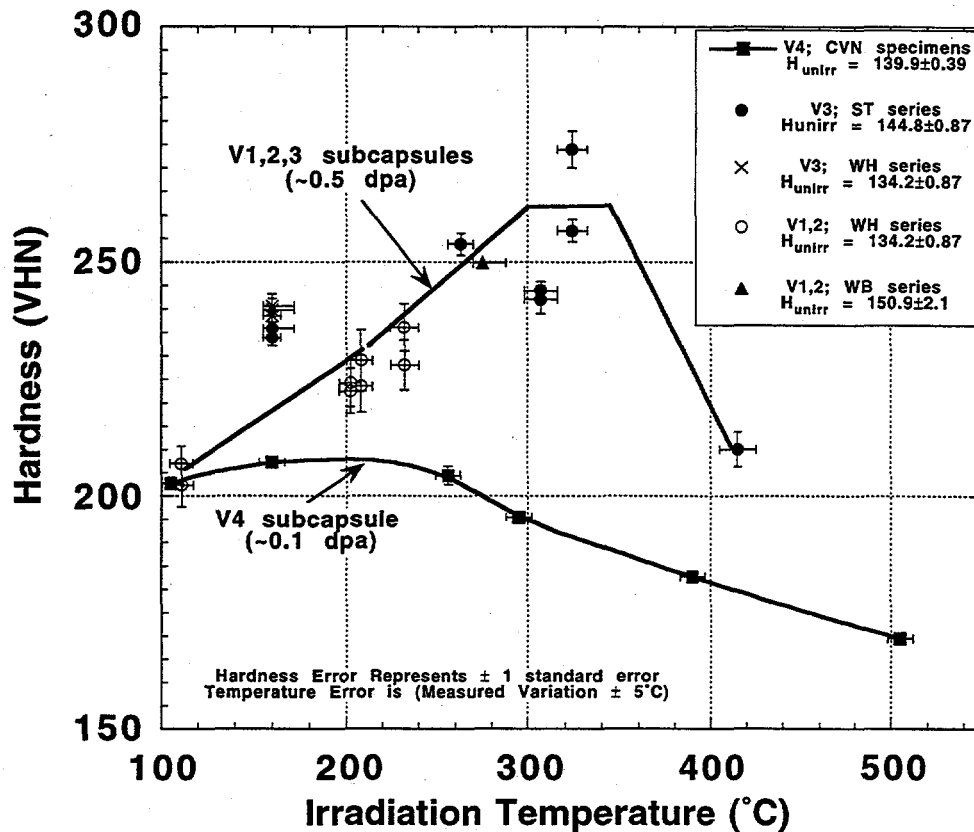


Fig. 2. Microindentation hardness of V-4Cr-4Ti irradiated in the HFBR.

Electrical Resistivity

The room temperature resistivity of the unirradiated control and irradiated tensile specimens was measured prior to tensile testing, using standard 4-point probe techniques (ASTM B 193-87, Standard Test Method for Resistivity of Electrical Conductor Materials, reapproved 1992). An electrical current of 100 mA was supplied by a Keithley Model 237 Source Measure Unit through spring-loaded electrical contacts located in the end tab regions of the tensile specimens. The potential drop in the gage region of the specimen was measured between two spring-load electrical contacts that were separated by a distance of 7.1 mm with a Keithley Model 182 Sensitive Digital Voltmeter with a low thermal connector (resolution limit of 1 nV). Potentials associated with thermal emfs in the electrical leads were subtracted using the "relative" reading function of the model 182 voltmeter. A minimum of three different tensile specimens were measured for each irradiation temperature. The typical measured resistances were ~ 1.5 - 1.8 m Ω . For capsules V2-V4, resistivity measurements were performed on the same specimens before and after irradiation in order to minimize errors associated with nonuniformities in the gage dimensions. The postirradiation measurements performed on specimens in the V1 capsule were compared with unirradiated measurements performed on sibling control specimens. The gage dimensions were measured to an accuracy of ± 2 μm in two different locations using a Mitotoyo digital micrometer in order to convert the resistance measurements to resistivity values. The

experimental error in the resistivity measurements was mainly due to uncertainties in the gage cross-sectional area; the typical measured standard error was ± 0.7 n Ω -m. The temperature was recorded for each measurement (20-26°C), and the data were corrected to a reference temperature of 20°C using the V-Cr-Ti alloy resistivity temperature coefficient [6] of 0.75 n Ω -m/K.

From Fig. 3 it is seen that the room-temperature resistivity increased by about 9 n Ω -m for irradiation at 108°C as compared to the unirradiated value of 280 n Ω -m. The increase in resistivity at this temperature is solely due to generation of point defect clusters in the lattice, since 108°C is too low for O, C, or N migration in vanadium [6-9]. As the irradiation temperature is increased for both the 0.1 and 0.5 dpa irradiated specimens, the change in resistivity decreases to zero (no change) at approximately 200°C and appears to reach a relative minimum of approximately -5 n Ω -m for irradiation temperatures near 300°C. Electron microscopy performed on the irradiated vanadium specimens found no change in the defect cluster size or density in the 110 to -275°C range [3,10], indicating that the decrease in resistivity in this temperature interval is not due to decreased defect cluster density. Using the measured migration enthalpies of C, O, and N in vanadium and V-4Cr-4Ti of ~1.18 eV, ~1.26 eV and ~1.48 eV, respectively [7-9], and the low-temperature defect cluster densities of ~0.3 to $1 \times 10^{23}/\text{m}^3$ [3,10], migration of C and O solute to defect clusters would be predicted to become significant at temperatures above ~150°C during the one to four week HFBR irradiation and N solute migration to defect clusters would be expected at temperatures above ~250°C. Therefore, the decrease in resistivity with increasing irradiation temperature between 100 and 300°C may be due to the formation of interstitial solute-point defect clusters (the resistivity associated with a solute-defect cluster complex would be less than the resistivity of isolated solute and defect clusters). The formation of the solute-point defect complexes would produce an increase in the dislocation barrier strength compared to point defect clusters without solute atoms, as is well-known from radiation anneal hardening studies [7,11]. Increased room temperature hardness and tensile strength was observed in the present study for specimens irradiated to 0.5 dpa at ~160-300°C compared to 110°C (cf. Fig. 2 and Table 3). Therefore, both the resistivity and hardness data suggest that interstitial solute strengthening of defect clusters may be occurring in V-4Cr-4Ti specimens irradiated at temperatures between ~160 and 300°C. At irradiation temperatures above ~300°C, the resistivity change begins to increase for both the 0.1 and 0.5 dpa irradiated specimens. This may be due to the decrease in defect cluster density (i.e., lower sink strength for interstitial solutes) as the irradiation temperature is raised above 300°C [10]. For the case of the 0.1 dpa irradiated material, the change in resistivity is seen to become slightly positive for an irradiation temperature of 504°C.

The observation that the resistivity did not increase dramatically at irradiation temperatures up to 504°C indicates that the measured low-temperature radiation hardening was not due to solution hardening from pickup of O or C interstitial solutes from the surrounding environment. The specific resistivities for O, C, and N solutes in vanadium are ~50 to 90 n Ω -m/at.% solute [6]. Therefore, the incorporation of a significant (>1000 appm; >300 wppm) amount of O or C in the matrix as solid solution impurities would have caused an easily detected (>5 n Ω -m) increase in the resistivity, which according to Fig. 3 did not occur in the irradiated specimens at temperatures where interstitial solutes are mobile in vanadium (>150°C). For irradiation temperatures above 300°C, the microstructure gradually evolved from small defect clusters to larger, lower density titanium rich clusters [10]. These larger defects would be less efficient sinks for migrating solutes and would therefore have less of an effect on reducing the resistivity. This TEM observation is in agreement with the trends towards higher resistivity seen in Fig. 3 and the reduced hardening seen in Fig. 2.

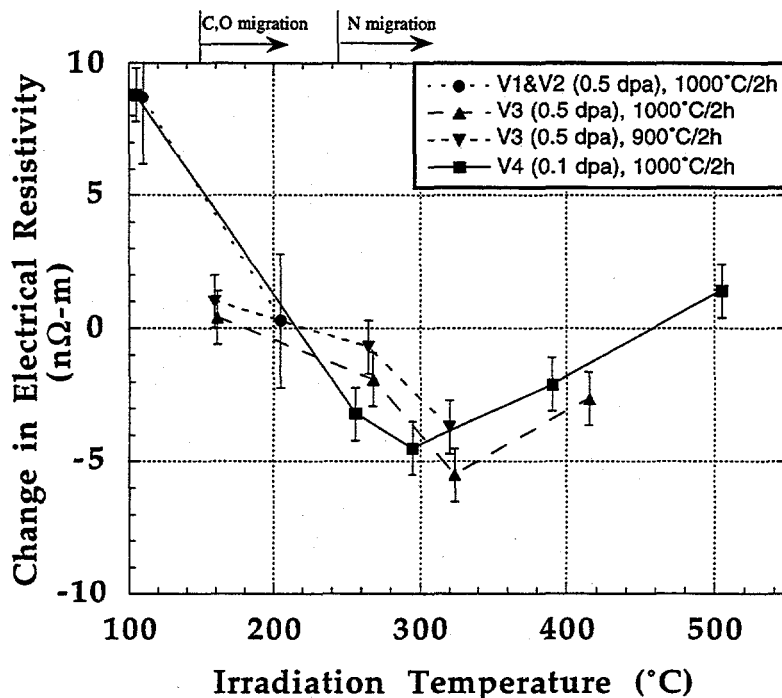


Fig. 3. Change in electrical resistivity of V-4Cr-4Ti irradiated in the HFBR.

Tensile Properties

The tensile specimens from the HFBR V1-V4 experiments were tested at ambient temperature in air or in vacuum at the irradiation temperatures. The majority of the samples were tested at a cross head speed of 0.02 or 0.05 inch/minute, corresponding to a strain rate of 10^{-3} s^{-1} . Three of the 0.1 dpa tensile specimens (capsule V4) were tested at 20°C with a shoulder-loaded specimen grip system, whereas all of the other specimens were tested using a standard pin-loading grip system. Slight deformation in the shoulder regions of the shoulder-gripped tensile specimens caused a change in the slope of the stress-strain curve prior to yielding in the gage region, and introduced a ~1% absolute error in the tensile elongation measurements for these three specimens.

Figure 4 shows examples of the stress-strain curves generated for the 0.5 dpa irradiated specimens tested at the irradiation temperature ($T_{\text{test}} \sim T_{\text{irr}}$). The offset in crosshead displacement is added for clarity. From the figure it is seen that a complete loss in strain hardening capacity has occurred for the specimens irradiated at 110-325°C. Similar behavior was also observed for the room temperature tests of specimens irradiated at 110-325°C.

The data for all tensile specimens included in the HFBR V1-V4 irradiation program are given in Table 3. Because low-temperature neutron irradiation produced a pronounced decrease in strain hardening capacity, the criterion for yielding used for these specimens is given in Fig. 5. For irradiation temperatures less than ~300°C, there is essentially no uniform elongation and therefore the 0.2% plastic deformation convention is inappropriate. For the cases, as indicated in Fig. 5, where there is <0.2% offset prior to a load drop, the yield strength is assigned to be the lower yield point which is given by the intersection of the lines drawn through the yield drop and the subsequent necking. This is given by the symbol σ_y in the figure. The ultimate stress (σ_u) in

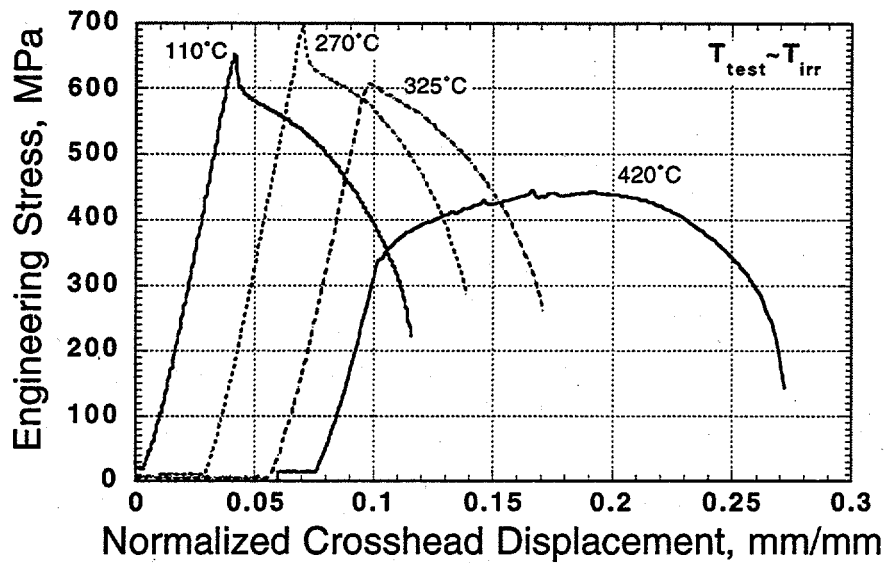


Fig. 4. Typical load vs. normalized crosshead displacement curves for V-4Cr-4Ti tensile specimens irradiated in the HFBR to 0.5 dpa.

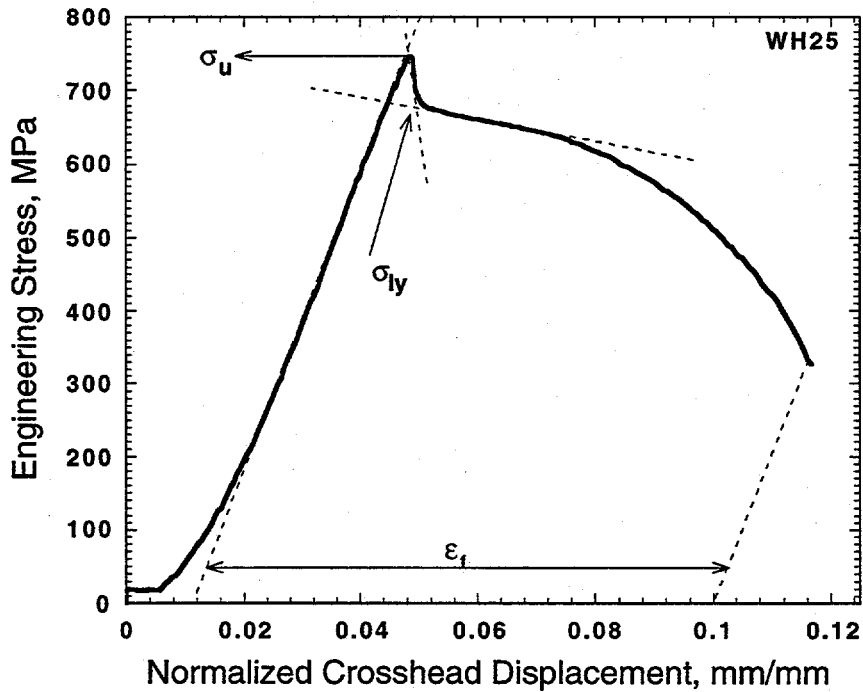


Fig. 5. Schematic illustrating how data were interpreted from the engineering tensile curves.

Table 3. Tensile data for the V-4Cr-4Ti specimens in HFBR V1-V4 capsules. All of the specimens were annealed for 2 h at 1000°C unless otherwise noted.

Sample ID	Capsule (sub-capsule)	Irrad. Temp. (°C)	Test Temp. (°C)	Strain Rate (inch/min)	Lower Yield Pt. (MPa)	Ultimate Stress (MPa)	Unif. Elong. (%)	Total Elong. (%)	Red. in Area (%)
WH01	V1 (4)	207	20	0.02	657	732	0	9.9	83
WH02	V1 (4)	207	200	0.02	603	652	0.05	8.7	
WH03	V1 (4)	207	20	0.002	655	672	0.67	10.3	
WH04	V2 (1)	232	240	0.02	591	657	0.05	9	
WH05	V2 (1)	232	20	0.02	705	769	0	9.7	
WH06	V2 (1)	232	240	0.02	589	623	0.1	8.8	
WH07	V2 (1)	232	240	0.05	635	676	0.1	9.4	
WH08	V2 (4)	203	200	0.02	580	650	0.05	9	
WH09	V2 (4)	203	20	0.02	661	695	0	9.3	80
WH10	V2 (4)	203	200	0.5	605	656	0.1	9.3	
WH11	V2 (4)	203	200	0.001	586	615	0.1	9	
WH13	V2 (5)	111	110	0.02	594	652	0.1	9.7	
WH14	V2 (5)	111	20	0.02	590	633	0	9	
WH15	V2 (5)	111	20	0.02	590	623	0.89	10.9	
WH23	V3 (1)	160	20	0.02	781	800	0.3	9	
WH25	V3 (1)	160	157	0.02	677	749	0.08	8.9	87
WH26-31	V3 (1)	160	untested						
WH32	V3 (1)	160	20	0.05	766	786	0.05	9	82
WH33-35	V3 (1)	160	untested						
ST12	V3 (1)	160	20	0.05	758	800	0	9.3	82
ST13-18	V3 (1)	160	untested						
ST45-48 [†]	V3 (1)	160	untested						
ST19	V3 (2)	268	20	0.05	795	859	0	8.8	85
ST20	V3 (2)	268	270	0.05	635	700	0	9.1	
ST21	V3 (2)	268	untested						
ST41 [†]	V3 (2)	268	untested						
ST22	V3 (3)	260	*						
ST23	V3 (3)	260	untested						
ST24	V3 (3)	260	*						
ST42 [†]	V3 (3)	260	untested						
ST25	V3 (4)	324	20	0.05	758**	761	0.05	9.3	87
ST26	V3 (4)	324	320	0.05	608**	608	0.1	9.5	
ST27	V3 (4)	324	untested						
ST43 [†]	V3 (4)	324	untested						
ST28	V3 (5)	307	20	0.05	733**	733	0	9	85
ST29	V3 (5)	307	untested						
ST30	V3 (5)	307	untested						
ST44 [†]	V3 (5)	307	untested						
ST31	V3 (6)	414	20	0.05	446**	530	11.8	21.7	73
ST32	V3 (6)	414	420	0.05	342**	445	5.9	19.6	
ST33-34	V3 (6)	414	untested						

Table 3 (continued): Summary of data for 0.1 dpa specimens.

Sample ID	Capsule (Sub-capsule)	Irrad. Temp. (°C)	Test Temp. (°C)	Strain Rate (inch/min)	Lower Yield Pt. (MPa)	Ultimate Stress (MPa)	Unif. Elong. (%)	Total Elong. (%)	Red. in Area (%)
ST53	V4 (1)	105	108	0.02	446**	515	1.4	11.9	
ST54	V4 (1)	105	20	0.02	578	593	<1.2 [§]	10	
ST55	V4 (1)	105	untested						
ST49 [†]	V4 (1)	105	untested						
ST59	V4 (3)	256	286	0.02	449	465	0.1	13	
ST60	V4 (3)	256	20	0.02	584	604	<1.2 [§]	12	
ST61	V4 (3)	256	untested						
ST51 [†]	V4 (3)	256	untested						
ST62	V4 (4)	294	340	0.02	393**	402	0.4	15.2	
ST63	V4 (4)	294	20	0.02	531	538	<1 [§]	14.3	
ST64	V4 (4)	294	290	0.02	422	437	0.1	13.6	
ST65	V4 (4)	294	untested						
ST66	V4 (5)	391	395	0.02	348	426	9	20.5	
ST67	V4 (5)	391	20	0.02	446	514	13.7	27.8	
ST68-69	V4 (5)	391							
ST57	V4 (6)	504	20	0.02	371**	503	19.2	24.4	
ST58	V4 (6)	504	untested						
ST71	V4 (6)	504	510	0.02	258**	420	11.2	22.7	
ST75	V4 (6)	504	untested						

*Sample damaged during capsule disassembly

**No load drop; table value represents 0.2% yield stress

[§]Shoulder loaded specimen; unreliable low-strain (<1%) elongation data

[†]2 h anneal at 900°C prior to irradiation

this case is by definition the stress at which the load drop occurs (i.e., upper yield point). For the cases where work hardening was present the same method was used to calculate σ_y , though the line through the "necking" region has either a near-zero or positive slope depending on the extent of the Luders band region. In the few cases where a yield drop was not observed (e.g. specimens irradiated to 0.5 dpa at 307-414°C), 0.2% plastic deformation was used for the yield strength as noted in Table 3.

Figure 5 also indicates the method used for determining the total (plastic) elongation, listed as ϵ_t in the figure. A note of caution regarding the uniform elongation for the low-temperature irradiated materials should be mentioned. For tensile curves exhibiting load-drop behavior with no subsequent work hardening (the majority of the data in Table 3), the uniform elongation was taken to be the elongation at maximum load. As this value is inherently low (<0.2%), the absolute error ($\leq 0.01\%$) is comparable to the measured value. In general, no significance should be placed on variations in the tabulated uniform elongations when the values are less than 0.2%.

Figure 6 shows the temperature-dependent strength at yielding for the unirradiated and irradiated specimens of this study. From the figure a substantial increase in the yield strength occurs at 0.1 dpa and increases further for the 0.5 dpa irradiation. Recent studies on V-4Cr-4Ti irradiated at temperatures of ~100-330°C indicate that the yield strength continues to increase up to doses of ~5 dpa [12-14], although additional data are needed at doses between 1 and 10 dpa to fully determine the dose dependence of the radiation hardening at low temperatures.

Figure 7 gives the uniform elongation for the 0.1 and 0.5 dpa irradiated V-4Cr-4Ti alloy tested at the irradiation temperature. It is clear from this figure that there is essentially no strain hardening capacity for this alloy for irradiation temperatures $\leq 324^\circ\text{C}$ at 0.5 dpa. For the 0.1 dpa irradiated

material there is a limited amount of uniform elongation (1.4%) for the 108°C irradiated specimen. However, as the irradiation temperature is increased, and C and O solutes can move to defect clusters, the material loses its strain hardening capacity and only ~0.1% uniform elongations were observed in specimens irradiated to 0.1 dpa at 256 and 294°C. After irradiation to 0.1 dpa at 391°C, the material exhibits high (9%) uniform elongation. It is clear from this plot that there is a lack of data in the very important irradiation temperature regime from ~300-500°C. Another significant aspect is that at irradiation temperatures up to at least 330°C this material has lost its strain hardening capacity at extremely low doses. This would seem to rule out the suggested [15] mitigating effects that fusion neutron-produced helium may have on the tensile elongations of vanadium alloys, at least for irradiation temperatures up to 330°C. Simply put, the amount of helium generated in a fusion reactor after a dose of ~0.5 dpa (~2 appm He) would be insufficient to have an impact (positive or negative) on the severe reduction in strain hardening capacity which occurs for fission reactor irradiation temperatures up to at least 330°C.

The reduction in area for a selected group of fractured tensile specimens was measured using scanning electron microscopy (SEM). The data from these specimens are summarized in Table 3 and indicate that the reduction in area was approximately 80% for all specimens regardless of whether they exhibited a severe reduction in strain hardening capacity (e.g., WH09), possessed limited uniform elongation (e.g., WH25), or had significant strain hardening capacity (e.g., ST31). An SEM micrograph of the fracture surface of a tensile specimen (WH01) irradiated to 0.5 dpa at 207°C is shown in Fig. 8. A higher magnification image of a tensile fracture surface is shown in Fig. 9, exhibiting ductile tearing in a sample which had essentially no uniform elongation.

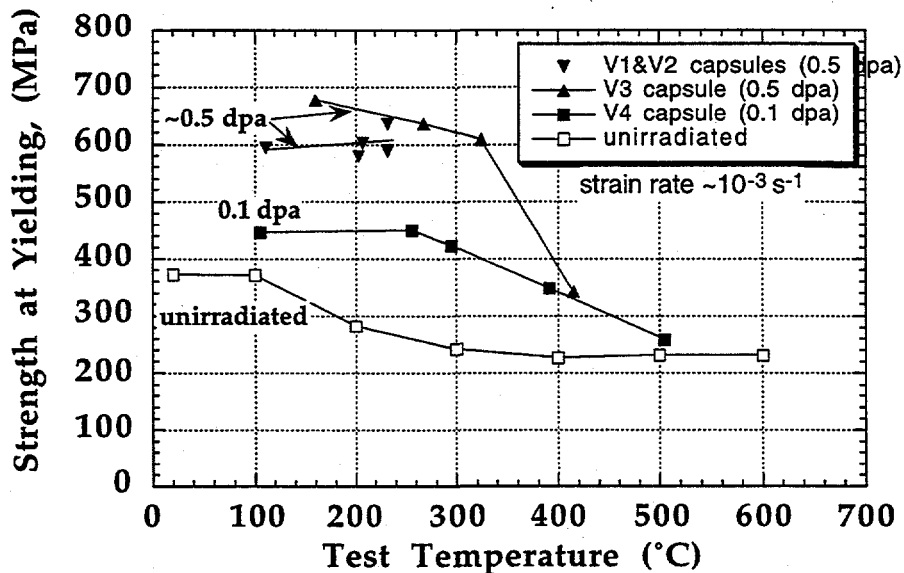


Fig. 6. Strength at yielding of V-4Cr-4Ti irradiated at low dose and low temperature in the HFBR (Testing temperature = Irradiation temperature).

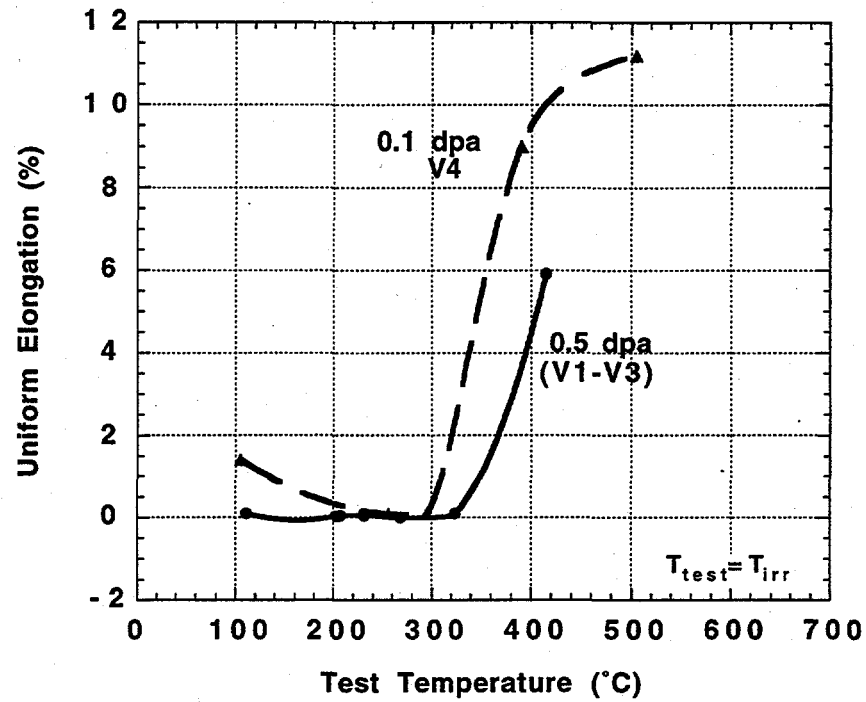


Fig. 7. Uniform elongations of V-4Cr-4Ti irradiated at low dose and low temperature in the HFBR. The tensile specimens were tested at the irradiation temperature.

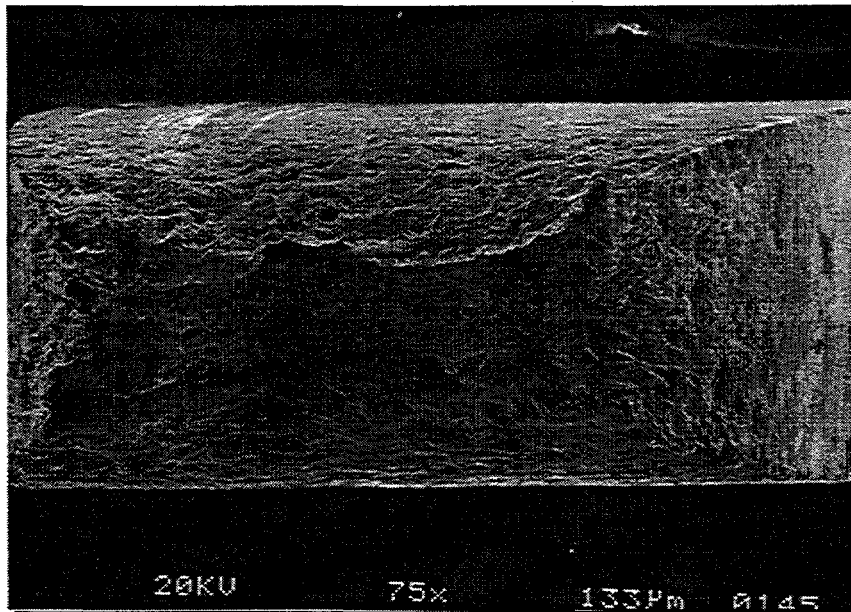


Fig. 8. Low magnification image of the fracture surface of a SS-3 sheet tensile specimen. Sample WH05 irradiated in HFBR-V2 to 0.5 dpa at 232°C and tested at room temperature.

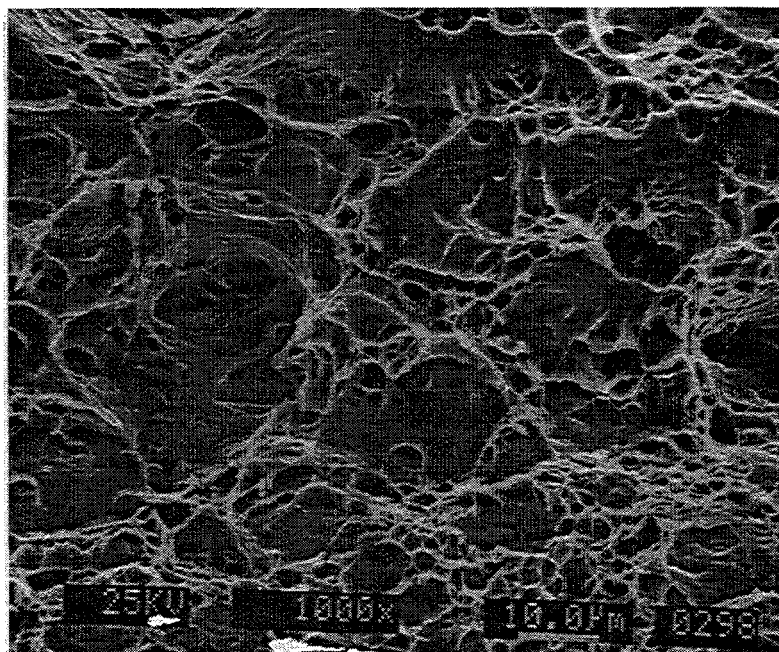


Fig. 9. High magnification image of the center of the fracture surface of a SS-3 sheet tensile specimen (Sample WH01, irradiated in HFBR-V1 to 0.5 dpa at 207°C and tested at 20°C).

Impact Testing

The subsized Charpy specimens (both machine-notched and pre-cracked) were tested in air on a pendulum machine modified for small specimens. Figures 10 and 11 give the absorbed energy data from these tests for the machined-notch (MCVN) and pre-cracked (PCVN) Charpy specimens, respectively. The unirradiated ductile to brittle transition temperature (DBTT) is seen from these figures to be $\sim 200^{\circ}\text{C}$ for the machined-notched specimens and $\sim 150^{\circ}\text{C}$ for the precracked specimens, indicating a notch acuity effect which has been previously seen in unirradiated vanadium alloys [1,12,16-18].

Figure 12 gives a summary of the DBTT for both the MCVN and PCVN specimens, indicating that the PCVN specimens exhibited DBTT values that were ~ 50 to 120°C higher than the corresponding MCVN specimens, with the largest deviations occurring when the measured DBTT's were relatively high. The largest shift in the DBTT for both types of Charpy samples correspond to the samples with near zero uniform elongation (Fig. 7 and Table 3). Other factors could contribute to the observed embrittlement such as (a) the inadvertent introduction of hydrogen during pre- or post-irradiation handling, and (b) the pick-up of oxygen and nitrogen from the capsule atmosphere during irradiation. As indicated from the section on electrical resistivity, mechanism (b) can be ruled out. Several of the irradiated CVN specimens were annealed in vacuum for 1 h at 400°C to remove hydrogen which may have been picked up by the specimens. Similar impact behavior was observed in the as-irradiated and annealed specimens, indicating that significant hydrogen pickup had not occurred [4].

Figures 13 and 14 give high magnification SEM images of fracture surfaces from the lower shelf and upper shelf samples. In both the PCVN and MCVN specimens, the upper shelf fracture surface showed ductile tearing. By stereoscopic imaging of the fracture surface of lower shelf specimens, the failure mode was seen to be cleavage, with some evidence of mixed-mode failure in the transition region from lower to upper shelf behavior.

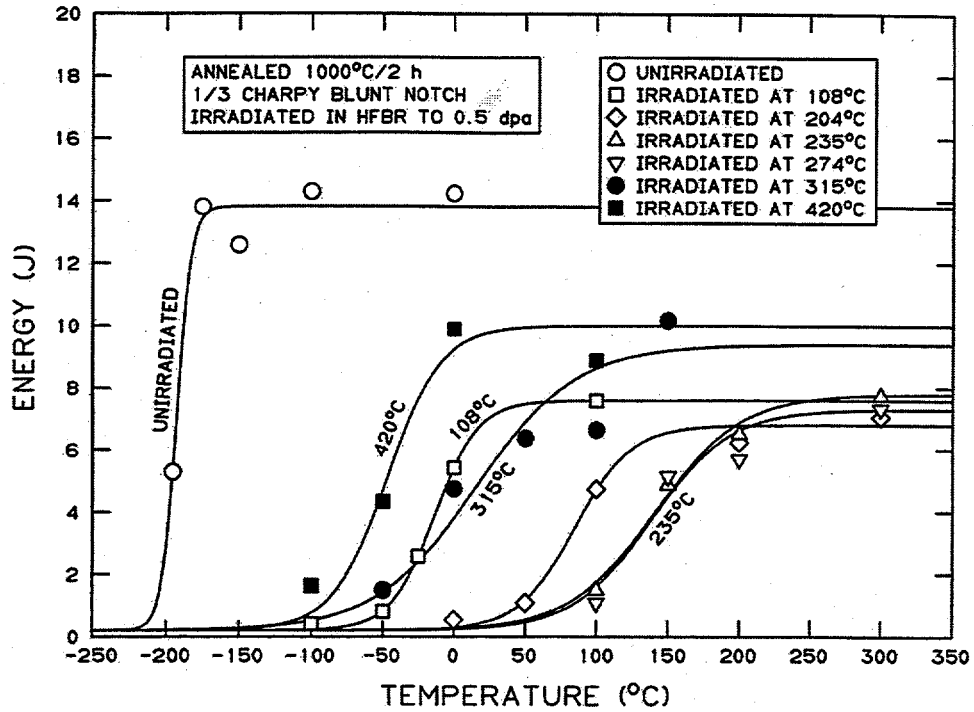


Fig. 10. Plot of the unirradiated and 0.5 dpa absorbed energy data for the impact testing of the machined-notch Charpy impact specimens (MCVN)

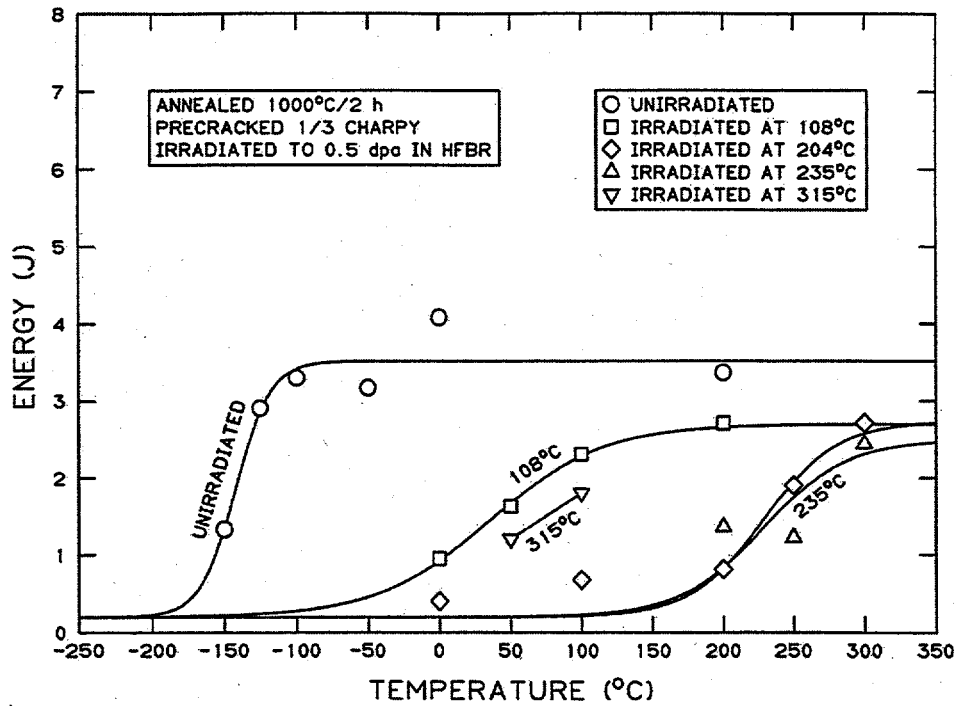


Fig. 11. Plot of the unirradiated and 0.5 dpa absorbed energy data for the impact testing of the pre-cracked Charpy impact specimens (PCVN).

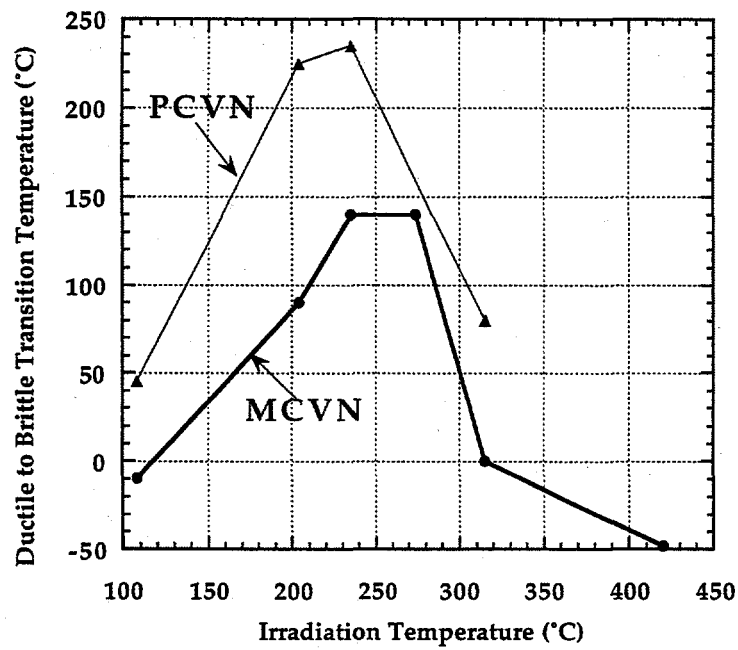


Fig. 12. Ductile to Brittle Transition Temperature for the machined-notch and pre-cracked Charpy specimens irradiated to 0.5 dpa.

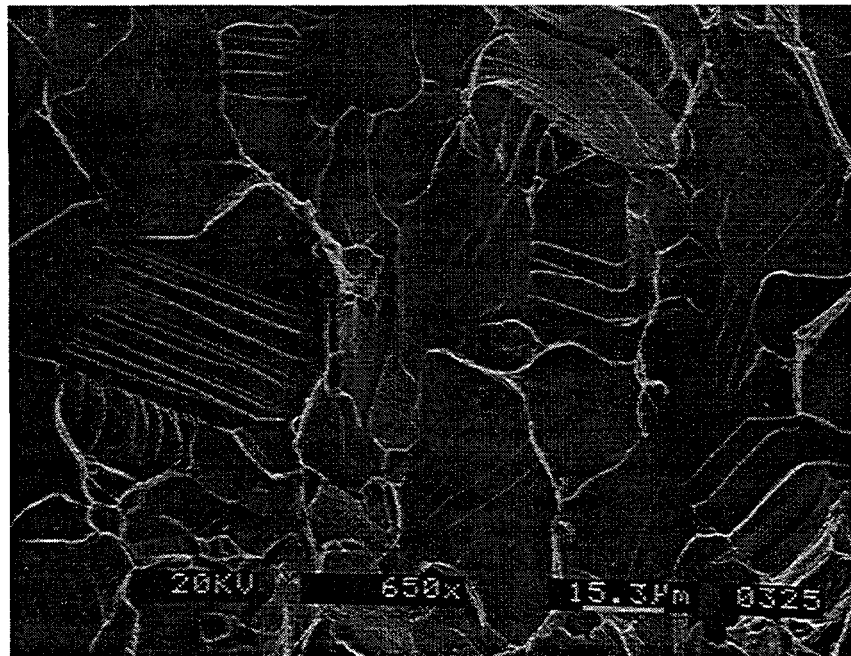


Fig. 13. SEM of the fracture surface from a 0.5 dpa PCVN specimen exhibiting lower shelf behavior (sample WB81, irradiated at 110°C and tested at 0°C).

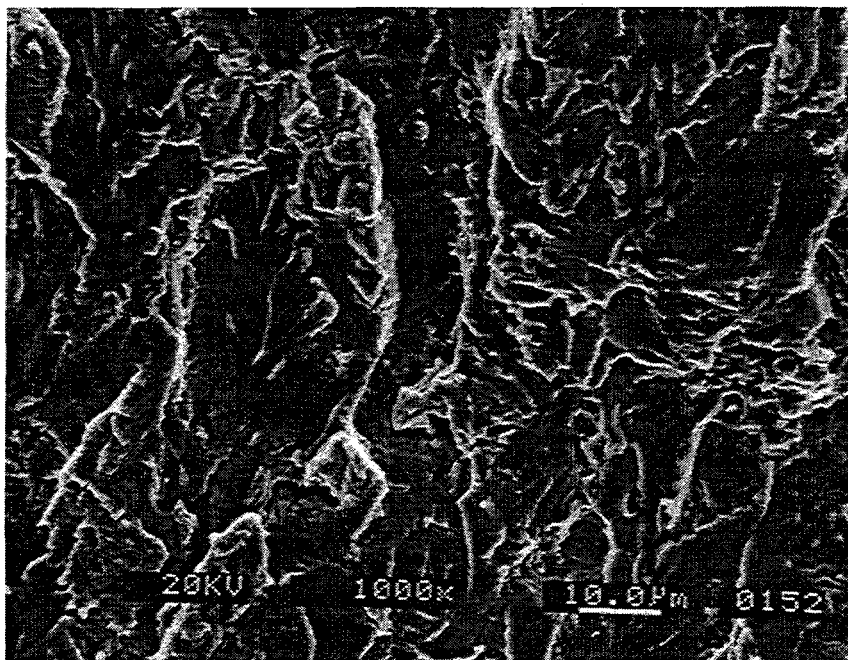


Fig. 14. SEM of the fracture surface from a 0.5 dpa Charpy specimen exhibiting behavior intermediate between upper and lower shelf. (Sample WB100, irradiated at 235°C and tested at 250°C).

CONCLUSIONS

Significant hardening of V-4Cr-4Ti with a corresponding increase in tensile strength, complete loss of strain hardening capacity, and a large increase in the DBTT has occurred for irradiation temperatures at or below 324 °C at 0.5 dpa. This embrittlement is due to the high density of radiation produced defect clusters which are further strengthened by migrating C, O and N interstitial solutes for fission reactor irradiation temperatures greater than ~150°C (C,O) and ~250°C (N), respectively. Irradiation at temperatures of 391-414°C to doses of 0.1-0.5 dpa produced reduced amounts of hardening and improved ductility compared to the low-temperature irradiations uniform elongation. A significant sensitivity of the ductile to brittle transition temperature on notch acuity has been observed in the irradiated Charpy specimens. Additional mechanical properties data on specimens irradiated at 300-500°C to higher fluences are required in order to establish the minimum operating temperature for this alloy.

FUTURE WORK

The majority of the post-irradiation testing of specimens from the HFBR V1-V4 irradiation experiment has been completed. Additional tasks which are planned include (a) the effect of strain rate on the tensile properties of the specimens irradiated at 160°C to 0.5 dpa, (b) isochronal annealing of low temperature irradiated specimens from HFBR-V1 to measure the recovery of microindentation hardness, (c) measurement of the electrical resistivity change for control specimens annealed in helium at 504°C for 1 to 4 weeks to investigate the extent of oxygen pickup, and (d) static fracture toughness testing on precracked HFBR V3 and V4 bend bars at temperatures up to 505°C. Some mechanical testing of the 900°C heat treated tensile and impact specimens (Table 3) will also be performed. Fracture mechanics testing of irradiated PCVN specimens is in progress at UC-Santa Barbara.

ACKNOWLEDGMENTS

The authors would like to give their sincere thanks to Joe O'Connor, Joel Errante, Guy Hartsough, Norman Holden, and Tim Powers of the Research Coordination Group of the Brookhaven National Laboratory for their cooperation and assisting in using the High Flux Beam Reactor. We would also like to thank Marie Williams and Jeff Bailey for assistance with the post irradiation evaluation of these samples.

REFERENCES

1. M.L. Grossbeck, A.F. Rowcliffe, and D.J. Alexander, in Fusion Materials Semiann. Prog. Report for Period ending March 31, 1994, DOE/ER-0313/16 (Oak Ridge National Lab, 1994) p. 244.
2. H.M. Chung et al., in Fusion Materials Semiann. Prog. Report for Period ending Sept. 30, 1994, DOE/ER-0313/17 (Oak Ridge National Lab, 1994) p. 178.
3. P.M. Rice, L.L. Snead, D.J. Alexander, and S.J. Zinkle, in Microstructure Evolution During Irradiation, MRS Symposium Proceedings vol. 439, eds. I.M. Robertson et al. (Materials Research Society, Pittsburgh, 1997) p. 343.
4. D.J. Alexander et al., in 18th ASTM Symp. on Effects of Radiation on Materials, Hyannis, MA, 1996, in press; also Fusion Materials Semiann. Prog. Report for Period ending June 30, 1996, DOE/ER-0313/20 (Oak Ridge National Lab, 1996) p. 87.
5. L.R. Greenwood and R.T. Ratner, in Fusion Materials Semiann. Prog Rep. for period ending Dec. 31 1997, DOE/ER-0313/23, in press.
6. S.J. Zinkle, A.N. Gubbi, and W.S. Eatherly, in Fusion Materials Semiann. Prog. Report for Period ending December 31, 1996, DOE/ER-0313/21 (Oak Ridge National Lab, 1996) p. 15.
7. J.T. Stanley, J.M. Williams, W.E. Brundage, and M.S. Wechsler, *Acta Metall.* 20 (1972) 191.
8. H. Nakajima, S. Nagata, H. Matsui, and S. Yamaguchi, *Philos. Mag. A* 67 (1993) 557.
9. M. Uz, K. Natesan and V.B. Hang, *J. Nucl. Mater.* 245 (1997) 191.
10. P.M. Rice and S.J. Zinkle, 8th Int. Conf. on Fusion Reactor Materials, Sendai, *J. Nucl. Mater.* (1998) submitted.
11. R.E. Gold and D.L. Harrod, *Intern. Metals Rev.* 25, no. 5-6 (1980) 232.
12. S.J. Zinkle et al., 8th Int. Conf. on Fusion Reactor Materials, Sendai, *J. Nucl. Mater.* (1997) submitted.
13. E.V. van Osch, 8th Int. Conf. on Fusion Reactor Materials, Sendai, *J. Nucl. Mater.* (1997) submitted.
14. V.A. Kazakov, V.P. Chakin, Y.D. Goncharenko, and Z.E. Ostrovsky, 8th Int. Conf. on Fusion Reactor Materials, Sendai, *J. Nucl. Mater.* (1997) submitted.
15. H.M. Chung, M.C. Billone, and D.L. Smith, in Fusion Materials Semiann. Prog. Report for Period ending June 30, 1996, DOE/ER-0313/22 (Oak Ridge National Lab, 1997) p. 22.
16. H. Li, R.H. Jones, and J.P. Hirth, in Fusion Materials Semiann. Prog. Report for Period ending March 31, 1994, DOE/ER-0313/16 (Oak Ridge National Lab, 1994) p. 279.
17. G.R. Odette, E. Donahue, G.E. Lucas, and J.W. Sheckherd, in Fusion Materials Semiann. Prog. Report for Period ending June 30, 1996, DOE/ER-0313/20 (Oak Ridge National Lab, 1996) p. 11.
18. G.R. Odette, G.E. Lucas, E. Donahue, and J.W. Sheckherd, *J. Nucl. Mater.* 233-237 (1996) 502.